

The Dependence of Scanning Tunneling Microscope Topography of Carboxylates on Their Terminal Groups

Akira Sasahara,* Hiroshi Uetsuka, Taka-aki Ishibashi, and Hiroshi Onishi

Surface Chemistry Laboratory, Kanagawa Academy of Science and Technology, KSP East 404, 3-2-1 Sakado, Takatsu-ku, Kawasaki 213-0012, Japan

Received: July 29, 2003; In Final Form: September 10, 2003

Carboxylate (RCOO^-) molecules with different terminal groups ($\text{R} = \text{H}$, CH_3 , $(\text{CH}_3)_3\text{C}$, $\text{HC}\equiv\text{C}$, and CF_3) adsorbed on an atomically flat $\text{TiO}_2(110)$ surface were observed by a scanning tunneling microscope (STM). The carboxylates were identified molecule by molecule as spots of different heights in microscope images obtained at positive sample bias voltage. The observed height of the carboxylates agreed with the spatial distribution of the unoccupied orbitals localized on each terminal group.

Introduction

Imaging adsorbed molecules has been an important subject in surface chemistry and has been achieved by use of a scanning tunneling microscope (STM).¹ Forthcoming molecule-scale devices for electrical applications should be based on a full understanding of electron transport through individual molecules adsorbed on solid surfaces.² In the present study, the STM topography of substituted carboxylates (RCOO^-) was examined with the terminal group R systematically substituted in the range of H, CH_3 , CF_3 , $(\text{CH}_3)_3\text{C}$, and $\text{HC}\equiv\text{C}$. The observed topography was related to the spatial distribution of molecular orbitals responsible for the electron tunnel.

An atomically flat surface of TiO_2 was utilized to prepare the well-characterized monolayer of the carboxylates. The (110) surface of the rutile TiO_2 provides the nonreconstructed truncation as illustrated in Figure 1 when prepared in an ultrahigh vacuum.^{3,4} This surface contains the row of Ti^{4+} cations and the row of O^{2-} anions lying parallel to the [001] direction. A carboxylic acid molecule (RCOOH) is dissociatively adsorbed as a carboxylate anion and a proton to present a long-range ordered monolayer at room temperature.^{5,6} Experimental^{7–9} and theoretical^{10,11} studies have revealed that formate ($\text{R} = \text{H}$) and acetate ($\text{R} = \text{CH}_3$) are adsorbed on a pair of Ti^{4+} cations with the C–R bond perpendicular to the surface. Carboxylates adsorbed in this bridge form provide a molecule-scale standard to compare the microscope topography of substituted terminal groups. The molecule-dependent topography of the carboxylates has been determined by noncontact atomic force microscope (NC-AFM).^{12–15}

Experimental Section

Experiments were carried out by using an ultrahigh vacuum microscope (JSPM-4500A, JEOL) equipped with an Ar^+ sputtering gun (IG35, OCI), low-energy electron diffraction optics (BDL600, OCI), and an X-ray photoelectron spectrometer (TM50045, JEOL). The base pressure of the microscope was below 3×10^{-8} Pa.

A $\text{TiO}_2(110)$ wafer ($7 \times 1 \times 0.3 \text{ mm}^3$, Shinko-sha) was clamped with a Si wafer for resistive heating. The (1×1) surface

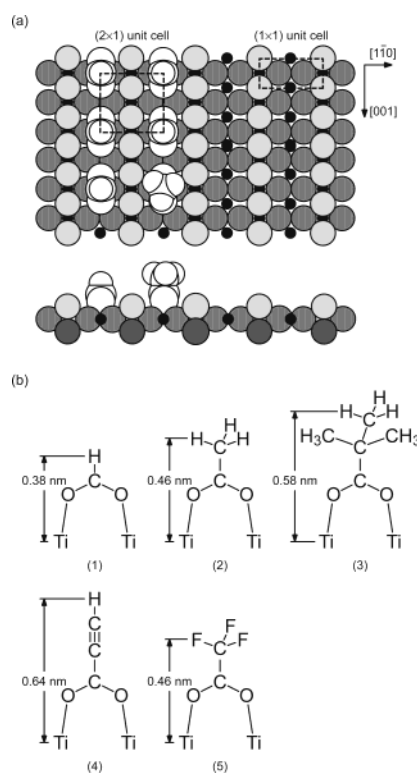


Figure 1. The models of substrate and molecules employed. (a) The $\text{TiO}_2(110)-(1 \times 1)$ surface and adsorbed molecules. Small and large spheres represent Ti and O atoms, respectively. Oxygen atoms are shaded according to their depth. Rectangles with dotted lines show unit cells. (b) The atom geometry of (1) formate, (2) acetate, (3) pivalate, (4) propiolate, and (5) trifluoroacetate adsorbed on the $\text{TiO}_2(110)$ surface.

was prepared by repeated Ar^+ sputtering and vacuum annealing at 900 K. The temperature of the wafer was monitored by an infrared pyrometer (TR630, Minolta). Contamination left on the sputter-annealed surface was under the detection limit of X-ray photoelectron spectroscopy. Carboxylic acid gas was purified by several freeze–pump–thaw cycles and dosed to the TiO_2 surface in the microscope. STM imaging was done in a constant current mode with a conductive Si cantilever (NSCS11, NT-MDT) as a probe. The dimension of the microscope image was calibrated on the lattice spacing and single step of the $\text{Si}(111)-$

* To whom correspondence should be addressed: Phone: +81-44-819-2048. FAX: +81-44-819-2095. E-mail: ryo@net.ksp.or.jp.

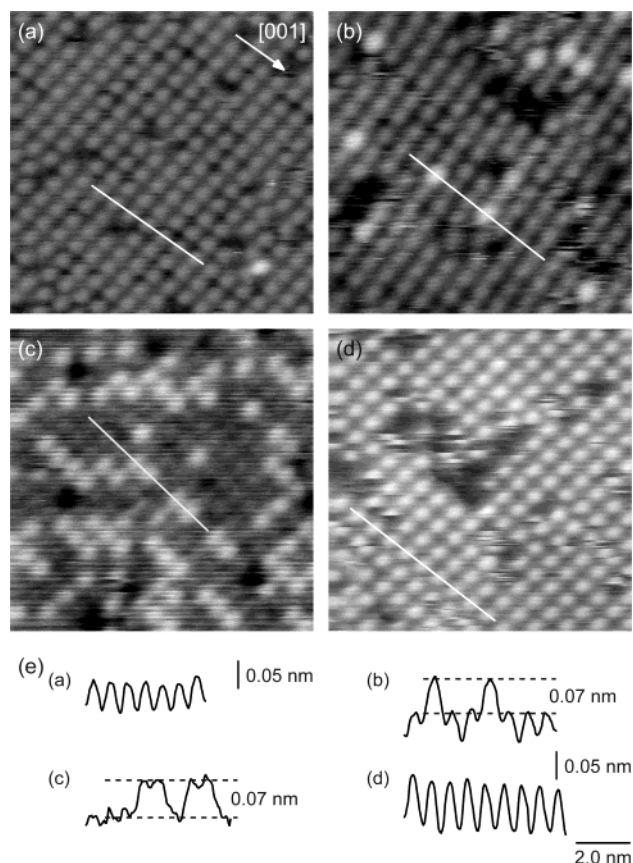


Figure 2. Constant current images of the TiO_2 surfaces covered by carboxylates ($10 \times 10 \text{ nm}^2$): (a) pure formate monolayer, (b) formate monolayer exposed to 0.1 L of acetic acid gas, (c) formate monolayer exposed to 1.5 L of acetic acid gas, and (d) pure acetate monolayer. Cross sections determined along the lines in the images are presented in panel e. Sample bias voltage (V_s) = +1.0 V, tunneling current (I_t) = 1.0 nA.

(7×7) surface. All images are presented without filtering. Cross sections were measured after a nine-point median operation.

Results and Discussion

Panels a and d in Figure 2 show the STM images of the pure formate monolayer and pure acetate monolayer. Individual formates and acetates were observed as spots with a regular height arranged in a (2×1) periodicity. Vacant sites where the carboxylate was not adsorbed were observed as dark patches. The fluctuation of the height was $\pm 0.01 \text{ nm}$ as shown in the cross sections. Each molecule had an oval topography elongated normal to the [001] direction.

When the formate-covered surface was exposed to the acetic acid gas, some of the formates were replaced by acetates.^{12,16} The STM images of the formate-covered surface exposed to 0.1 and 1.5 L (1 L = 10^{-6} Torr s) of the acetic acid gas are shown in Figure 2, panels b and c, respectively. Since the number of bright spots increased with the exposure time, they were assigned to the acetate. The formates and acetates maintained the (2×1) arrangement, which indicated that both carboxylates were adsorbed with the bridge configuration in the mixed monolayer. The difference in height between the formate and acetate was determined to be 0.07 nm from the cross section.

Panels a and b in Figure 3 are the STM images of the formate-covered and acetate-covered surfaces exposed to pivalic acid ($(\text{CH}_3)_3\text{CCOOH}$) gas. Bright spots and nonbright spots were ordered in the (2×1) periodicity. Each bright spot, which increased in number with exposure time, was assigned to pivalate.

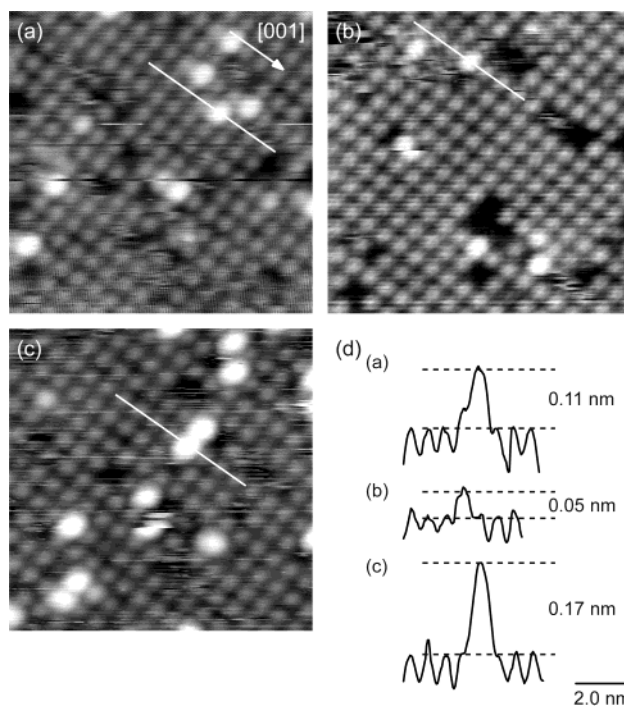


Figure 3. Constant current images of the mixed monolayers composed of (a) formate and pivalate, (b) acetate and pivalate, and (c) formate and propiolate ($10 \times 10 \text{ nm}^2$). Cross sections determined along the lines in the images are presented in panel d. V_s = +1.0 V, I_t = 1.0 nA.

The cross sections in Figure 3d show that the pivalate protruded by 0.11 nm from the formate monolayer and by 0.05 nm from the acetate monolayer. The height difference between the formate and acetate was hence indirectly determined to be 0.06 nm, which was consistent with the number directly obtained in the mixed monolayers of the formate and acetate, 0.07 nm. Thus the observed vertical topography of the formate, acetate, and pivalate was reproducible and free from the tip-dependent artifacts. Figure 3c is the STM image of the formate-covered surface exposed to propiolic acid ($\text{HC}\equiv\text{CCOOH}$) gas. The bright spots were assigned to the propiolates in a similar manner. The propiolate was 0.17 nm higher than the formate.

The mixed monolayer of the acetate and trifluoroacetate was prepared by exposing the $\text{TiO}_2(110)$ surface partially covered with trifluoroacetate to acetic acid gas, because the trifluoroacetate hardly replaced the preadsorbed acetates. Figure 4a is an STM image of the $\text{TiO}_2(110)$ surface exposed to 3 L of trifluoroacetic acid gas. The surface was covered with oval spots, whose apparent height was uniform except for the four bright spots indicated by arrows. The ratio of the bright spots, nonbright spots, and vacant sites to the entire adsorption site was 0.02, 0.60, and 0.38. When this surface was exposed to 0.3 L of acetic acid gas, the bright spots increased in number as shown in Figure 4b. The ratio of the bright and nonbright spots in Figure 4b was 0.14 and 0.67. Vacant sites decreased to 0.19 in the ratio and the spots were arrayed in the (2×1) long-range order. When the surface was exposed to an additional 3.3 L of acetic acid gas, the surface was almost covered with molecules as shown in Figure 4c. The ratio of the bright spots increased to 0.40 while the number of nonbright spots was constant, 0.58. The ratio of the vacant sites decreased to 0.02. Thus the bright spots were assigned to the acetates which filled the vacant sites in the trifluoroacetate-covered surface. The four bright spots in Figure 4a were assumed to be acetates adsorbed from acetic acid gas emitted from the chamber wall.

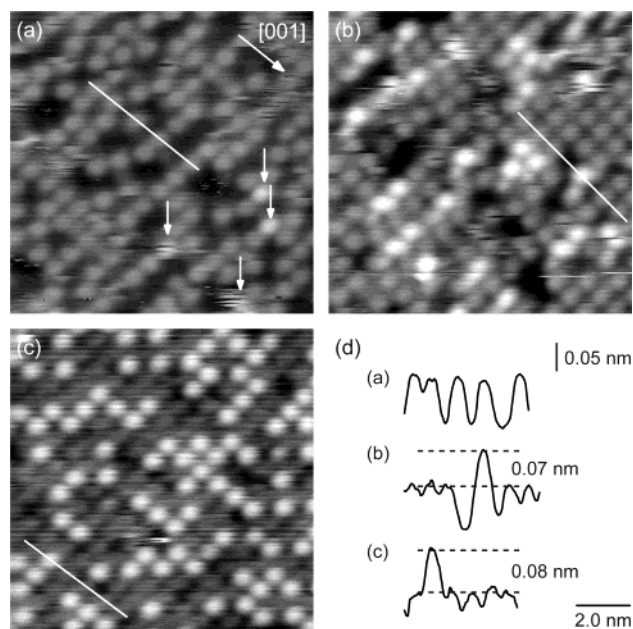


Figure 4. Constant current images of the TiO_2 surfaces covered by carboxylates ($10 \times 10 \text{ nm}^2$): (a) the TiO_2 surface exposed to 3 L of trifluoroacetic acid gas, (b) the surface shown in panel a exposed to 0.3 L of acetic acid gas, and (c) the surface shown in panel b exposed to 3.3 L of acetic acid gas. Cross sections determined along the lines in the images are presented in panel d. $V_s = +1.0 \text{ V}$, $I_t = 1.0 \text{ nA}$.

We ascribed the observed molecule-dependent topography to the spatial distribution of the molecular orbital that contributed to the electron tunnel from the tip. It has been revealed that ad molecules have characteristic image shapes reflecting their molecular orbitals.^{17–19} The molecular orbitals of the adsorbed carboxylates were calculated with $(\text{RCOO}^-)_2\text{-Ti}_2\text{O}_2(\text{OH})_2$ clusters, where each carboxylate was bound to the two Ti atoms. The restricted Hartree–Fock calculation with a 6-31G(d,p) basis function was performed by using the Gaussian 98 package.²⁰ Figure 5a shows the energy-optimized structure of the $(\text{HCOO}^-)_2\text{-Ti}_2\text{O}_2(\text{OH})_2$ cluster, where the Cartesian coordinate system was defined with its y axis perpendicular to the O–C–O plane of the formate. The OCO angle and Ti–O

distance of the carboxylates in the clusters were predicted to be 127° and 0.21 nm being consistent with the accepted values.^{8,10,11}

The observed microscope topography of the individual carboxylates was oval and elongated perpendicular to the [001] direction. This characteristic feature of the adsorbed carboxylate was originally found on $\text{HCOO/TiO}_2(110)$ and interpreted with the electron tunnel into the lowest unoccupied molecular orbital (LUMO) of the adsorbate.⁶ The LUMO of an HCOO^- isolated in space is an antibonding π^* state composed of $2p_y$ orbitals of the carbon and two oxygen atoms. If the molecular orbital closest to the tip apex dominates the electron tunnel across the STM gap, which is a reasonable assumption, the lateral distribution of the LUMO around the carbon atom is reproduced in the STM topography. That was indeed the case of the formate. The $2p_y$ orbitals expanded perpendicular to the O–C–O plane and reproduced the observed lateral topography of the formate.

We extended this interpretation to the four other carboxylates examined in the present study. The unoccupied molecular orbital located within 5 eV from the LUMO and containing the largest contribution of the $2p_y$ orbital of the carboxy carbon was selected from each cluster. They are illustrated in Figure 5b–f with their energy eigenvalues. The vertical height in the STM topography was qualitatively reproduced with the surface plot of the orbitals chosen.

Trifluoroacetate provided a complicated case. The spatial distribution of the orbital raised in Figure 5f can reproduce the reduced STM height of the fluorine-substituted acetate when compared with the normal acetate. The fluorine atoms in CF_3 contributed to the molecular orbital to a lesser extent than the hydrogen atoms in CH_3 did. The atomic orbitals of the fluorines were energetically separated away from the rest of the atomic orbitals and contributed little to the molecular orbital. In addition, the permanent dipole moment of the CF_3 terminal perturbed the tunnel barrier. Tunnel current I at tip–surface distance s is approximated with barrier height Φ and bias voltage V as²¹

$$I \approx V \exp(-\Phi^{0.5}s) \quad (1)$$

When a surface is covered with electric dipole moments μ oriented from the vacuum toward the surface with a density σ ,

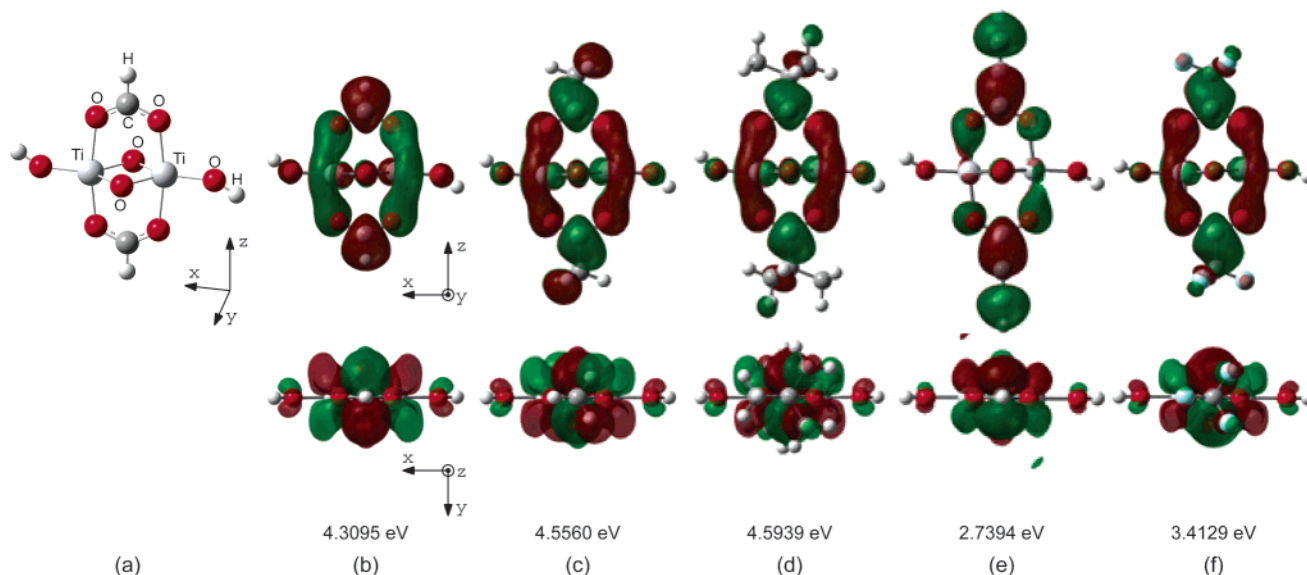


Figure 5. (a) The ball-and-stick model of the $(\text{HCOO}^-)_2\text{-Ti}_2\text{O}_2(\text{OH})_2$ cluster after structure optimization. Surface plot of the unoccupied orbital of the $(\text{RCOO}^-)_2\text{-Ti}_2\text{O}_2(\text{OH})_2$ clusters ($0.02 \text{ bohr}^{-1.5}$): (b) $\text{R} = \text{H}$, (c) $\text{R} = \text{CH}_3$, (d) $\text{R} = (\text{CH}_3)_3\text{C}$, (e) $\text{R} = \text{HC}\equiv\text{C}$, (f) $\text{R} = \text{CF}_3$. The upper and lower plots are side and top views, respectively. The molecular orbitals of the plus and minus phase are brown and green, respectively.

$$\Phi = \phi + e\mu\sigma/\epsilon_0 \quad (2)$$

where ϕ and ϵ_0 are the barrier height of the unperturbed surface and permittivity in a vacuum. The dipole moment of a free HCF_3 molecule, which was determined at 1.65 D (1 D = 3.34×10^{-30} C m),²² provides an estimate of the moment on the CF_3 group terminating the trifluoroacetate. By putting $\mu = 1.65$ D and $\sigma = 2.6 \times 10^{18} \text{ m}^{-2}$ in (2), the barrier height is increased by 1.6 eV. When the unperturbed barrier height is assumed to be 4 eV, eq 1 requires s to be reduced by 15% to maintain the current at a fixed voltage. With a standard tip–surface distance of 1 nm, a reduction of 0.15 nm is thereby predicted. On the other hand, CF_3 -terminated acetates isolated in the monolayer of the CH_3 -terminated acetate exhibited an STM topography reduced by 0.07–0.08 nm (Figure 4). The smaller perturbation observed on an isolated molecule was consistent with the prediction that was made for the moments densely packed along the (2×1) order.

In summary, carboxylates terminated with six different alkyl groups were chemisorbed on the atomically flat surface of rutile TiO_2 and visualized by STM. The observed microscope topography of individual carboxylates was related to the molecular orbitals predicted on the model cluster. The topography of the CF_3 -terminated acetate can further be perturbed by its electric dipole moment via the increased height of the tunnel barrier.

Acknowledgment. This work was supported by Core Research for Evolutional Science and Technology (CREST) from the Japan Science and Technology Corporation (JST).

References and Notes

- (1) Wiesendanger, R. *Scanning Probe Microscopy and Spectroscopy*; Cambridge University Press: New York, 1994.
- (2) Adams, D. M.; Brus, L.; Chidsey, C. E. D.; Creager, S.; Creutz, C.; Kagan, C. R.; Kamat, P. V.; Lieberman, M.; Lindsay, S.; Marcus, R. A.; Metzger, R. M.; Michel-Beyerle, M. E.; Miller, J. R.; Newton, M. D.; Rolison, D. R.; Sankey, O.; Schanze, K. S.; Yardley, J.; Zhu, X. *J. Phys. Chem. B* **2003**, *107*, 6668.
- (3) Henrich, V. E.; Cox, P. A. *The Surface Science of Metal Oxides*; Cambridge University Press: New York, 1994.
- (4) Diebold, U. *Surf. Sci. Rep.* **2003**, *48*, 53.
- (5) Onishi, H. In *Chemistry of Nanomolecular Systems*; Nakamura, T., Matsumoto, T., Tada, H., Sugiura, K., Eds.; Springer-Verlag: Berlin, Germany, 2003; p 75.
- (6) Onishi, H.; Iwasawa, Y. *Chem. Phys. Lett.* **1994**, *226*, 111.
- (7) Guo, Q.; Cocks, I.; Williams, E. M. *J. Chem. Phys.* **1997**, *106*, 2924.
- (8) Thevuthasan, S.; Herman, G. S.; Kim, Y. J.; Chambers, S. A.; Peden, C. H. F.; Wang, Z.; Ynzunza, R. X.; Tober, E. D.; Morais, J.; Fadley, C. S. *Surf. Sci.* **1998**, *401*, 261.
- (9) Gutiérrez-Sosa, A.; Martínez-Escobedo, P.; Raza, H.; Lindsay, R.; Wincott, P. L.; Thornton, G. *Surf. Sci.* **2001**, *471*, 163.
- (10) Bates, S. P.; Kresse, G.; Gillan, M. J. *Surf. Sci.* **1998**, *409*, 336.
- (11) Käckell, P.; Terakura, K. *Surf. Sci.* **2000**, *461*, 191.
- (12) Sasahara, A.; Uetsuka, H.; Onishi, H. *Appl. Phys. A* **2001**, *72* [Suppl.], S101.
- (13) Sasahara, A.; Uetsuka, H.; Onishi, H. *Surf. Sci.* **2001**, *481*, L437.
- (14) Sasahara, A.; Uetsuka, H.; Onishi, H. *Appl. Surf. Sci.* **2002**, *188*, 265.
- (15) Sasahara, A.; Uetsuka, H.; Onishi, H. *Phys. Rev. B* **2001**, *64*, 121406(R).
- (16) Uetsuka, H.; Sasahara, A.; Yamakata, A.; Onishi, H. *J. Phys. Chem. B* **2002**, *106*, 11549.
- (17) Nejoh, H. *Appl. Phys. Lett.* **1990**, *57*, 2907.
- (18) Lipple, P. H.; Wilson, R. J.; Miller, M. D.; Wöll, Ch.; Chiang, S. *Phys. Rev. Lett.* **1989**, *62*, 171.
- (19) Ohtani, H.; Wilson, R. J.; Chiang, S.; Mate, C. M. *Phys. Rev. Lett.* **1988**, *60*, 2398.
- (20) Frisch, M. J.; Trucks, G. W.; Schlegel, H. B.; Scuseria, G. E.; Robb, M. A.; Cheeseman, J. R.; Zakrzewski, V. G.; Montgomery, J. A., Jr.; Stratmann, R. E.; Burant, J. C.; Dapprich, S.; Millam, J. M.; Daniels, A. D.; Kudin, K. N.; Strain, M. C.; Farkas, O.; Tomasi, J.; Barone, V.; Cossi, M.; Cammi, R.; Mennucci, B.; Pomelli, C.; Adamo, C.; Clifford, S.; Ochterski, J.; Petersson, G. A.; Ayala, P. Y.; Cui, Q.; Morokuma, K.; Salvador, P.; Dannenberg, J. J.; Malick, D. K.; Rabuck, A. D.; Raghavachari, K.; Foresman, J. B.; Cioslowski, J.; Ortiz, J. V.; Baboul, A. G.; Stefanov, B. B.; Liu, G.; Liashenko, A.; Piskorz, P.; Komaromi, I.; Gomperts, R.; Martin, R. L.; Fox, D. J.; Keith, T.; Al-Laham, M. A.; Peng, C. Y.; Nanayakkara, A.; Challacombe, M.; Gill, P. M. W.; Johnson, B.; Chen, W.; Wong, M. W.; Andres, J. L.; Gonzalez, C.; Head-Gordon, M.; Replogle, E. S.; Pople, J. A. *Gaussian 98*, Revision A.11; Gaussian, Inc.: Pittsburgh, PA, 2001.
- (21) Spong, J. K.; Mizes, H. A.; LaComb, L. J., Jr.; Dovek, M. M.; Frommer, J. E.; Foster, J. S. *Nature* **1989**, *338*, 137.
- (22) Lide, D. R., Ed. *CRC Handbook of Chemistry and Physics*, 81st ed.; CRC Press: Boca Raton, FL, 2000.